

## Dynamics of the $\alpha$ relaxation of a glass-forming polymeric system: Dielectric, mechanical, nuclear-magnetic-resonance, and neutron-scattering studies

J. Colmenero, A. Alegría, J. M. Alberdi, and F. Alvarez  
*Departamento de Física de Materiales, Facultad de Química,  
 Apartado 1072, 20080 San Sebastián, Spain*

B. Frick

*Institute Max von Laue–Paul Langevin (ILL), Grenoble, France*  
 (Received 29 April 1991; revised manuscript received 8 July 1991)

The dynamics of the  $\alpha$  relaxation in a glass-forming polymeric system, poly(vinyl methyl ether) (PVME) has been studied by means of dielectric and mechanical spectroscopies and nuclear magnetic resonance, as well as by means of quasielastic neutron scattering. By using these techniques we have covered a wide time scale ranging from mesoscopic to macroscopic times ( $10^{-10}$ – $10^1$  sec). The dielectric and mechanical data have been interpreted in terms of a Havriliak-Negami relaxation function,  $\Phi_{\text{HN}}$ . Nuclear-magnetic-resonance data were interpreted by means of a spectral density function  $J(\omega)$  based on  $\Phi_{\text{HN}}$ . Neutron-scattering data were described in terms of a scattering law  $S(Q, \omega)$  which was also built starting from  $\Phi_{\text{HN}}$ . The results obtained from different experimental techniques indicate that the dynamics of the  $\alpha$  relaxation in PVME can be well described by means of (i) a common temperature-independent spectral shape and (ii) a common temperature behavior of the relaxation times. We deduce for the spectral shape very similar parameters by fitting the Havriliak-Negami relaxation function to the different experimental data. These shape parameters are found to be not very sensitive to changes of temperature. The resulting characteristic relaxation times follow a Vogel-Fulcher-like temperature behavior in the temperature range  $T_g - 5 \text{ K} < T < T_g + 150 \text{ K}$ . Therefore, this implies a self-consistent description of the dynamics of the  $\alpha$  relaxation obtained by very different probes in PVME.

### I. INTRODUCTION

During recent years, a great deal of effort has been made in the study of the dynamics of the  $\alpha$  relaxation in very different glass-forming systems (ionic, low molecular weight, polymers, etc.) (see Refs. 1–4 as general references). From the results obtained it appears that the  $\alpha$ -relaxation behavior is universal, i.e., it does not depend on the glass-forming system considered. The dynamics of the  $\alpha$  relaxation is directly related to the liquid-glass transition. A “transition” which still remains open to controversy despite the great effort recently made from both the theoretical and experimental point of view.

The main experimentally established features of the dynamics of the  $\alpha$  relaxation can be summarized as follows.

The dynamics of the  $\alpha$  relaxation shows stretching, i.e., the complex susceptibility associated with a given excitation displays a clear non-Debye frequency behavior. This is characterized by a half-width of the susceptibility loss peak which is larger than 1.14 decades, the value corresponding to a Debye peak. In the time domain this corresponds to a stretched, nonexponential time decay.

The  $\alpha$  relaxation shows scaling behavior. This means that the normalized susceptibility spectrum corresponding to a given excitation is a temperature-independent function when the frequency  $\omega$  is rescaled by a characteristic time scale  $\tau(T)$ ,  $\omega_r = \omega\tau(T)$ . Similar behavior is found in the time domain for the corresponding correlation function. In this case the magnitude which should

be rescaled is the time  $t_r = t/\tau(T)$ . Therefore, the temperature dependence of the  $\alpha$  relaxation only enters via the temperature dependence of the characteristic time scale  $\tau(T)$ .

The characteristic time scales  $\tau(T)$  obtained from different probes follow a non-Arrhenius temperature behavior which is unusual in physics. In general, this behavior can be parametrized by means of the empirical Vogel-Fulcher law, although some deviations are noted in the high-temperature range as well as when  $T$  approaches the experimental glass-transition temperature  $T_g$ . With respect to this, another interesting point is completely open to controversy, whether or not the characteristic time scales obtained by different probes behave with temperature in a similar way. If this universality is confirmed, the relaxation phenomena observed by different techniques should be different projections of the same structural relaxation mechanism.

We want to point out that almost all of these features have been established by means of different spectroscopies (e.g., standard dielectric and mechanical spectroscopies or photon correlation spectroscopy) in the frequency range, say  $f \leq 10^7$  Hz down to macroscopic frequencies. However, almost nothing is known about how the above-mentioned signatures of the  $\alpha$  relaxation translate to rather microscopic frequency range between  $10^7$  and  $10^{12}$  Hz (mesoscopic range). Recently, the mode-coupling theory, describing the dynamics of simple supercooled liquids,<sup>5–7</sup> predicted stretching and scaling

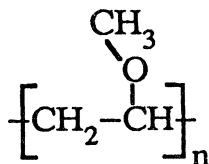
for the  $\alpha$  resonance peaks as well as universality for the characteristic time scales of this process at the mesoscopic frequency range which is the relevant range for this theory. Some of these predictions have been checked during the last two or three years by means of neutron scattering in different glass-forming systems (see as representative Refs. 8–12, and references therein). In general, stretching and scaling of the  $\alpha$  relaxation have been found at the mesoscopic range for all the systems investigated. Also, there is some evidence that the shift factor  $a(T)$  used to build a master curve for the intermediate scattering function  $I(Q, t)$  behaves with temperature such as the shear viscosity. However, a systematic comparison of the above-mentioned features of the  $\alpha$  relaxation in the mesoscopic/macrosopic range, using different spectroscopies, has not been made up to date.

We have performed a complete and careful study of the  $\alpha$  relaxation in a glass-forming polymeric system by several techniques covering a wide frequency range from macroscopic to microscopic frequencies between  $10^{-2}$  and  $10^{11}$  Hz, applying dielectric and mechanical spectroscopies, nuclear magnetic resonance and quasielastic neutron scattering. As a glass-forming system we have investigated poly (vinyl methyl ether) (PVME). This system has several advantages. First of all it does not crystallize, allowing us to explore a wide temperature range above  $T_g$  without any problem. It also has a comfortable  $T_g$  of 250 K and a high dielectric moment, thus allowing dielectric spectroscopy measurements. In addition, although it is not a main chain polymer, the monomer has quite a simple chemical structure. On the other hand, the dynamics of its side group (methyl side group) was previously studied by neutron scattering<sup>13</sup> which resulted in a very fast process ( $\tau \sim 10^{-12}$  s) and was apparently uncoupled to the  $\alpha$  relaxation.

## II. EXPERIMENT

### A. Sample

PVME from Polysciences Inc., average molecular weights  $\bar{M}_n = 37\,000$  and  $\bar{M}_w = 63\,000$ , were purified using benzene as the solvent and *n*-hexane as the precipitating agent. The glass transition  $T_g$  of the purified sample as measured by differential scanning calorimetry was 250 K. The chemical formula of the repeating unit is



### B. Dielectric measurements

The dielectric measurements covered the frequency range from 5 to  $10^5$  Hz. The measurement system uses a lock-in amplifier EG&G PAR 5208 with an internal oscillator, allowing a frequency range between 5 Hz and 100 Hz to be covered. The stray capacitance of the cell

was reduced to  $10^{-14}$  F. The sample was kept between two condenser aluminum plates that were held at a fixed distance. The capacitance of the sample cell was of the order of  $10^{-11}$  F. A standard 10 pF air capacitor was used as a reference in order to minimize errors in dielectric loss measurements, so the experimental limit for the loss factor value was about  $10^{-4}$ . The measurements were performed scanning the frequency at isothermal conditions at temperatures between 250 and 300 K. Then the real and imaginary parts of the dielectric susceptibility ( $\chi^* = \chi' - i\chi''$ ) were obtained as a function of frequency and temperature.

### C. Mechanical measurements

The dynamic mechanical behavior of PVME was studied by means of a standard Polymer Laboratories DMTA apparatus operating in the bending mode. Thus, we measured dynamic mechanical properties using flexural deformation and we obtained the real and imaginary components of the complex Young's modulus ( $E^* = E' + iE''$ ). The frequency range covered extends from 0.01 to 100 Hz. The experiments were performed at isothermal conditions in the temperature range between 243 and 273 K every 5 K.

### D. Nuclear magnetic resonance

NMR experiments were carried out on bulk PVME by means of a Varian VXR-300 spectrometer. Carbon spin-lattice relaxation times  $T_1$  and  $T_{1\rho}$  were measured at 75.4 MHz and 35.3 KHz, respectively, with a 10-mm probe by using the technique of proton noise decoupling. The experimental procedure used by us has been previously described.<sup>14</sup> Values of the relaxation times  $T_1$  and  $T_{1\rho}$  were obtained from exponential regression of the magnetization as a function of the recovery time. The temperature range covered in this study was from 330 to 410 K.

### E. Incoherent quasielastic neutron scattering

Neutron-scattering measurements were carried out by means of the neutron-backscattering spectrometers IN10 and IN13 at the Institute Laue Langevin (ILL) in Grenoble. The incident wavelengths used by us were  $\lambda = 6.28$  Å (IN10) and  $\lambda = 2.23$  Å (IN13), giving an energy resolution of  $\delta E \sim 1$   $\mu$ eV and  $\delta E \sim 8$   $\mu$ eV, respectively. The  $Q$  range covered by us was roughly between 0.2–2 Å<sup>-1</sup> on IN10 and 0.2–5.4 Å<sup>-1</sup> on IN13. The samples (thickness: 0.15 mm) were filled in a cylindrical Al container yielding a transmission of about 85%. The temperature range studied was from 250 to 350 K in the IN13 instrument and from 250 to 400 K in the case of the IN10 instrument. The typical measuring time at each temperature was 24 h for IN10 and 36 h for IN13. Initial data treatment was carried out in the normal way, correcting for effects of detector efficiencies, scattering from sample container, and instrumental background. The incoherent scattering experimental curve  $S(Q, \omega)$  was finally ob-

tained at each temperature as a function of the frequency change on scattering,  $\omega$ , and the modulus of the change of wave vector  $Q$ .

### III. RESULTS

#### A. Dielectric relaxation

We report first on the measurements of the dielectric susceptibility. Providing dielectric  $\alpha$  relaxation is a segmental movement which is perpendicular to the main chain, only the dipole moment of the monomeric unit in the direction perpendicular to the polymer chain should be relevant. For the PVME monomer it results to be 0.71 D (Ref. 15) which gives rise to quite an intense dielectric relaxation. The results we obtained for the normalized  $\chi''(\omega)$  at different temperatures are shown in Fig. 1a. As can be seen in this figure the shape of the dielectric relaxation function apparently does not change with temperature. However, in general, the frequency window covered at each temperature is not wide enough to define the whole  $\chi''(\omega)$  curve. Only around 260 K the loss curve is well defined. In this temperature range it is evident that

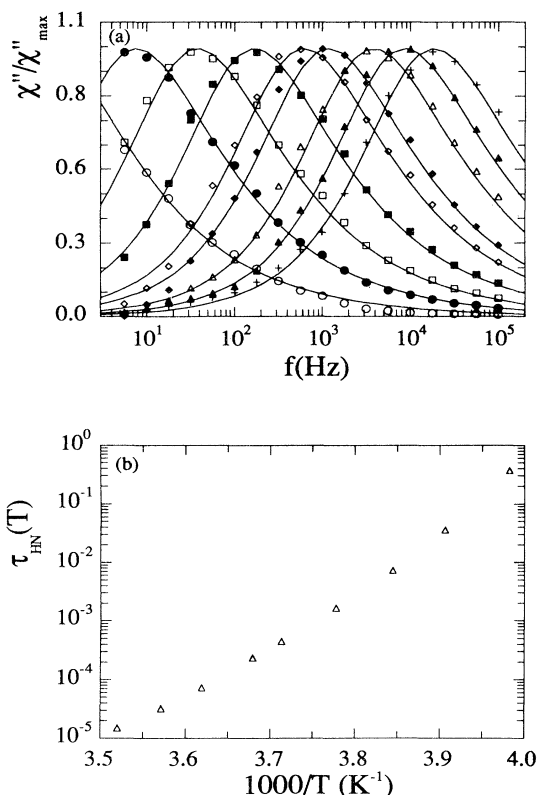


FIG. 1. (a) Normalized imaginary part of the dielectric susceptibility at 251.1 (○), 256.0 (●), 260.1 (□), 264.7 (■), 269.3 (◇), 271.8 (◆), 276.3 (△), 280.0 (▲), 284.1 K (+). The lines correspond to the HN fit with  $\alpha=0.65$  and  $\gamma=0.64$ . (b) Temperature dependence of the characteristic relaxation time  $\tau_{\text{HN}}$  obtained from the fitting of dielectric data.

the experimental  $\chi''(\omega)$  is much broader than the one corresponding to a simple Debye relaxation process (1.14 decades at one-half of the maximum) being moreover markedly asymmetric.

For the reasons given above the well-known Havriliak-Negami (HN) empirical relaxation function<sup>16</sup> was used to fit the data. The HN relaxation function can be written as

$$\Phi^*(\omega) = \frac{1}{[1 + (i\omega\tau_{\text{HN}})^\alpha]^\gamma}, \quad (1)$$

where  $\alpha$  and  $\gamma$  are two parameters in the range ( $0 < \alpha, \gamma < 1$ ) characterizing, respectively, the symmetric and asymmetric broadening, and  $\tau_{\text{HN}}$  is a characteristic time of the relaxation process. In the limit in which  $\alpha$  and  $\gamma$  take the value 1, Eq. (1) leads to a simple Debye law. The HN function is a generalization of the Cole-Cole<sup>17</sup> and Cole-Davidson<sup>18</sup> functions and gives rise to a high-frequency asymptotic behavior similar to the corresponding one of the von Schweidler law,<sup>7</sup> where the product  $\alpha\gamma$  corresponds to the von Schweidler exponent. Moreover, the time Fourier transformed of Eq. (1) shows a stretched exponential behavior, which can be well described by the Kohlrausch-Williams-Watts (KWW) law ( $\exp[-(t/\tau)^\beta]$ ).<sup>19,20</sup>

In the case of dielectric relaxation we can write the normalized relaxation function as

$$\frac{\chi^*(\omega) - \chi_u}{\chi_r - \chi_u} = \Phi^*(\omega), \quad (2)$$

where  $\chi_u$  and  $\chi_r$  are the unrelaxed and completely relaxed susceptibility, respectively. We have fitted the experimental data by Eqs. (1) and (2). First we have determined  $\alpha$  and  $\gamma$  around  $T=260$  K. Then we have fixed the obtained optimized values for the other temperatures and have thus determined the temperature dependence of  $\tau_{\text{HN}}$ . In Fig. 1 we show some dielectric susceptibility data. The solid lines in fig. 1(a) show the HN fitting curves corresponding to  $\alpha=0.65$  and  $\gamma=0.64$ , and the corresponding  $\tau_{\text{HN}}$  values are shown in Fig. 1(b). These values of the HN parameters are similar to those obtained by Kremer *et al.* ( $\alpha=0.65$  and  $\gamma=0.68$ ) for the dielectric  $\alpha$  relaxation of this polymer.<sup>21</sup> As expected, the  $\tau_{\text{HN}}(T)$  behavior shown in Fig. 1(b) is clearly non-Arrhenius and it will be discussed more extensively below.

#### B. Mechanical relaxation

Results from mechanical relaxation measurements are shown in Fig. 2. The frequency behavior of the normalized loss modulus  $E''(\omega)$  of PVME in the temperature range investigated is shown in Fig. 2(a). As in the case of dielectric losses the shape of  $E''(\omega)$  does not seem to change with temperature. Again the HN function was used to fit the experimental data. In this case the frequency dependence of the dynamic modulus can be written as

$$\frac{E_u - E^*(\omega)}{E_u - E_r} = \Phi^*(\omega), \quad (3)$$

where  $E_u$  and  $E_r$  are the unrelaxed and completely relaxed modulus, respectively. As in the case of dielectric data, the procedure followed was to find the values  $\alpha$  and  $\gamma$  that fit well the 248 K data (it is at this temperature when the mechanical loss peak is best defined). Then fixing the shape parameters we found the characteristic time  $\tau_{\text{HN}}$  values corresponding at all the temperatures investigated. As can be seen in Fig. 2(a) the mechanical dynamic behavior of PVME is also well described by means of the HN response function with the  $\alpha=0.69$  and  $\gamma=0.64$  shape parameters which are similar to those found for the dielectric relaxation. Again the corresponding values of  $\tau_{\text{HN}}(T)$  shown in Fig. 2(b) show a clear non-Arrhenius behavior that will be discussed more extensively below.

### C. Nuclear magnetic resonance

Because in this study we are interested in the main-chain dynamics, we have measured the spin-lattice relaxation times  $T_1$  and  $T_{1\rho}$  corresponding to the CH group in the main chain of PVME. The  $^{13}\text{C}$  peak corresponding to this group appeared as a well-defined peak in the spec-

trum at 75.2 ppm with reference to tetramethylsilane. The values obtained for  $T_1$  and  $T_{1\rho}$  have been plotted in Figs. 3(a) and 3(b) as a function of temperature.

With the assumption of a purely  $^{13}\text{C}$ - $^1\text{H}$  dipolar relaxation mechanism, the spin-lattice relaxation times  $T_1$  and  $T_{1\rho}$  obtained from  $^{13}\text{C}$  experiments are given by the usual expressions<sup>22</sup>

$$T_1^{-1} = \frac{\hbar^2 \gamma_C^2 \gamma_H^2}{10r_{\text{CH}}^6} [3J(\omega_C) + 6J(\omega_H + \omega_C) + J(\omega_H - \omega_C)], \quad (4a)$$

$$T_{1\rho}^{-1} = \frac{\hbar^2 \gamma_C^2 \gamma_H^2}{10r_{\text{CH}}^6} [2J(\omega_{C\rho}) + 1.5J(\omega_C) + 3J(\omega_H) + 3J(\omega_H + \omega_C) + 0.5J(\omega_H - \omega_C)]. \quad (4b)$$

In Eqs. (4a) and (4b),  $\omega_C$  and  $\omega_H$  are the Larmor frequencies for carbon and proton respectively,  $\omega_{C\rho}$  is the Lar-

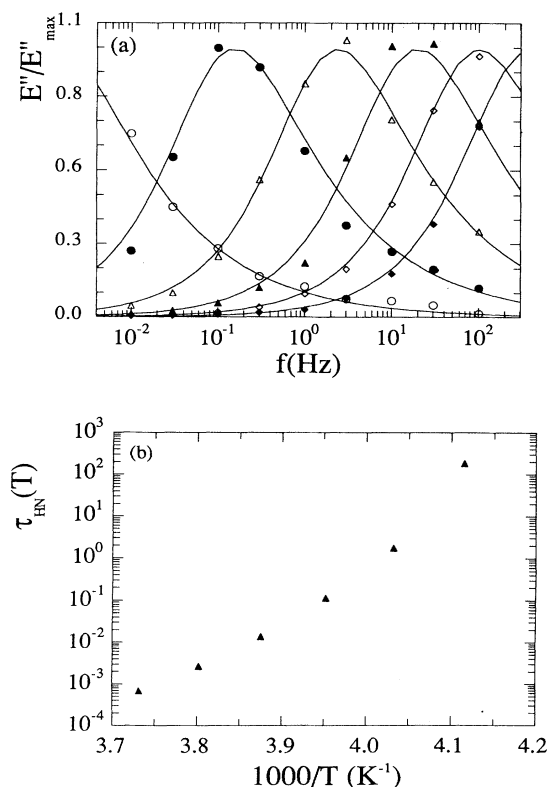


FIG. 2. (a) Normalized imaginary part of the complex dynamical modulus at 243 ( $\circ$ ), 248 ( $\bullet$ ), 253 ( $\triangle$ ), 258 ( $\blacktriangle$ ), 263 ( $\diamond$ ), and 268 K ( $\blacklozenge$ ). The lines correspond to the HN fit with  $\alpha=0.69$  and  $\gamma=0.64$ . (b) Temperature dependence of the characteristic relaxation time  $\tau_{\text{HN}}$  obtained from the fitting of mechanical data.

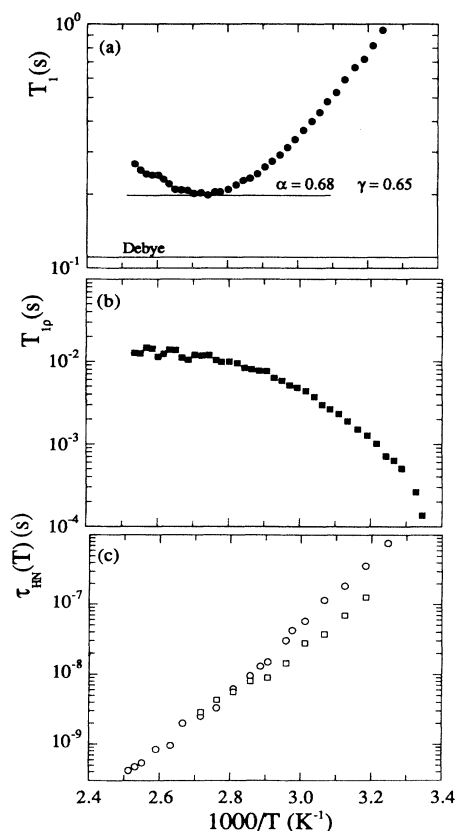


FIG. 3. (a) Temperature behavior of  $^{13}\text{C}$  spin-lattice relaxation times  $T_1$ . The value of the minimum of  $T_1(T)$  obtained by a HN spectral density function is shown in comparison with the expected one for a Debye process. (b) Temperature behavior of  $^{13}\text{C}$  spin-lattice relaxation times  $T_{1\rho}$ . (c) Temperature dependence of the characteristic relaxation times  $\tau_{\text{HN}}$  obtained from the fitting of  $T_1$  (circles) and  $T_{1\rho}$  (squares) data by means of the HN function with  $\alpha=0.68$  and  $\gamma=0.65$ .

mor frequency for the carbon in the radio-frequency field,  $\gamma_C$  and  $\gamma_H$  are the gyromagnetic ratios, and  $r_{CH}$  is the carbon-proton internuclear distance. For the CH group in the main chain of PVME we have used  $r_{CH} = 1.09 \text{ \AA}$ .<sup>23</sup>  $J(\omega)$  is the spectral density function which is defined as the one-side Fourier transform of the self-correlation function  $G(t)$  of the carbon-proton relative position. For a Debye process  $G(t)$  displays an exponential decay and  $J(\omega)$  is given by a Lorentzian  $J(\omega) = \tau(1 + \omega^2\tau^2)^{-1}$ . Under these conditions Eq. (4) predicts a value of 0.118 s for the  $T_1$  minimum corresponding to PVME at  $\omega_C/2\pi = 75.4 \text{ MHz}$  and  $\omega_H/2\pi = 299.9 \text{ MHz}$ . However, the experimental value obtained ( $0.206 \pm 0.01$ s) is much larger. A similar discrepancy of 75% with respect to the calculated value has also been found by Monnerie, Dejean de la Batie, and Lauprete<sup>23</sup>. This is expected for a nonexponential behavior of  $G(t)$ . Therefore, we describe again the  $T_1$  and  $T_{1\rho}$  experimental behavior by a spectral function  $J(\omega)$  derived from a Havriliak-Negami (HN) relaxation function. Thus,

$$J(\omega) = -\frac{1}{\omega} \text{Im}[\Phi^*(\omega)], \quad (5)$$

where  $\Phi^*(\omega)$  is the HN normalized relaxation function Eq. (1).

By means of Eqs. (1), (4a), (4b), and (5) it is possible for a given set of  $\alpha$  and  $\gamma$  parameters to obtain the values of the characteristic time  $\tau_{HN}(T)$  in the temperature range covered experimentally. However, the chosen values of  $\alpha$  and  $\gamma$  must yield an adequate value of  $T_1$  at the minimum and, moreover, have to give similar values of  $\tau_{HN}(T)$  obtained from both  $T_1$  and  $T_{1\rho}$  experiments. Values of  $\gamma = 0.65$  and  $\alpha = 0.68$  have proven to be adequate to match the  $T_1$  value at the minimum,  $T_1^{(\min)}$  (see Fig. 3). Also the  $T_1^{(\min)}$  values published by Monnerie, Dejean de la Batie, and Lauprete<sup>23</sup> at different frequencies, 62.5 and 25.15 MHz are well described. As shown in Fig. 3(c) the  $\alpha$  and  $\gamma$  values used also allow similar values for the characteristic times  $\tau_{HN}(T)$ , to be obtained from  $T_1$  and  $T_{1\rho}$  data. The temperature behavior of the Havriliak-Negami relaxation time  $\tau_{HN}$  obtained will be discussed below.

#### D. Quasielastic neutron scattering

Due to the fact that we used protonated samples we mainly observed the incoherent scattering arising from the self-correlation function which involves the motion of protons. In the  $\alpha$  relaxation range, the dynamics in PVME was detected by neutron scattering as a quasielastic broadening by IN10 and by IN13 at temperatures higher than 300 K. Figure 4(a) shows a typical spectrum in the IN10 window. In this figure it is clear that the experimental quasielastic data cannot be well described by a single Lorentzian function. This could again be considered as a consequence of the nonexponential behavior of the  $\alpha$  process in the time domain. Therefore, in order to fit the data we have built a scattering function  $S(Q, \omega)$  starting from the Havriliak-Negami frequency relaxation function, Eq. 1, as in the case of the NMR measurements. Thus,  $S(Q, \omega)$  can be expressed as

$$S(Q, \omega) \propto -\frac{1}{\omega} \text{Im}[\Phi^*(\omega)], \quad (6)$$

where  $\Phi^*(\omega)$  is the HN normalized relaxation function given by Eq. (1), but here, the  $\tau_{HN}$  values also depend on  $Q$ .

In order to test which values of the  $\alpha$  and  $\gamma$  shape parameters apply to the neutron-scattering range we have studied the variation of the mean-square deviation  $\sigma$  between theory and experimental data as a function of the product  $\alpha\gamma$  for some experimental spectra. We have chosen three spectra measured on IN10 at 375 K, which show simultaneously clear broadening and good statistics. We have only explored the parameter range of  $\alpha$  and  $\gamma$  corresponding to a stretched exponential behavior in time<sup>20</sup> ( $\alpha\gamma$  is close to  $\beta$ , the exponent of the KWW function). As can be seen in Fig. 4(a) at least for the tested temperature (375 K) and  $Q$  values a minimum in  $\sigma$  vs

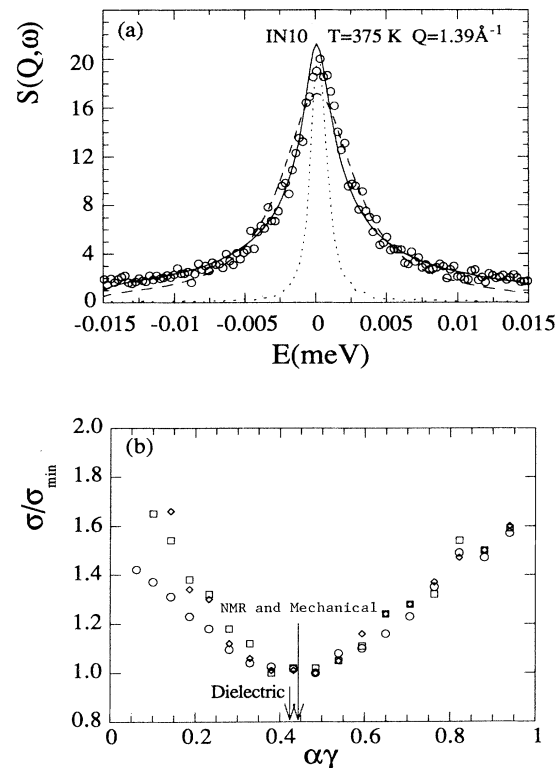


FIG. 4. (a)  $S(Q, \omega)$  of PVME measured by IN10. The dashed line corresponds to a single Lorentzian fit, the solid curve was obtained by the fitting of a HN function, Eq. (6), with  $\alpha = 0.68$  and  $\gamma = 0.65$ . The measured resolution is also shown for comparison (dotted line). (b) Normalized mean-square deviation of  $S(Q, \omega)$  from the fitting curve as a function of the product  $\alpha\gamma$ . These values correspond to the  $S(Q, \omega)$  measured in IN10 at 375 K, with  $Q$  values of 0.88 ( $\circ$ ), 1.18 ( $\square$ ), 1.39  $\text{\AA}^{-1}$  ( $\diamond$ ). The arrows indicate the values of  $\alpha\gamma$  corresponding to the HN parameters deduced from relaxation measurements.

$\alpha\gamma$  appears around  $\alpha\gamma=0.44$ , in good agreement with the parameters  $\gamma=0.65$  and  $\alpha=0.68$ , which we had found for the NMR measurements above. As the temperature range covered for NMR and neutron-scattering experiments are completely overlapped and, moreover, as both experimental techniques follow the dynamics of protons, this seems to be a reasonable result.

Figure 5 shows several experimental spectra obtained from IN10 and IN13 spectrometers. In the case of the IN13, it is clear from the high-energy tails of the experimental spectra that a nearly flat background is present. In the case of IN10 spectra this is not so evident mainly because of the limited energy window of this spectrometer. An experimental value of the flat background (FBG) can be easily determined from the data corresponding to the high energy tails of the IN13 spectra where the central component is not clearly broadened. However, when the broadening of the central component increases, the experimental determination of the FBG value becomes more difficult. In spite of these difficulties, values of the FBG were experimentally determined as described above in a wide  $Q$  range ( $0.2\text{--}2.5 \text{ \AA}^{-1}$ ) for all the temperatures investigated by the IN13 spectrometer. In this range the

broadening is not large enough to distort the high-energy tails behavior appreciably. The values of the flat background found by us do not appear to be very depending on  $Q$ .

The origin of such a FBG could be related to a very fast process with respect to the dynamical window of the spectrometer. In this case, only the central part of the process close to their maximum intensity would be detected by the instrument. At this range, this fast process should be approximately flat. This kind of process could include different possible contributions such as harmonic phonons, the additional fast process detected around  $T_g$  in several glasses,<sup>24,25</sup> and methyl group rotations.<sup>13</sup> The strength of all of these possible contributions should increase with  $Q$ . However, the broadening of such contributions should also increase with  $Q$ . Therefore, the intensity at the maximum could become hardly dependent on  $Q$  as we experimentally found.

Thus, starting from the chosen shape parameters and experimentally determined FBG, the values of the relaxation time  $\tau_{\text{HN}}(Q, T)$  were determined from the fitting of the experimental data of IN10 and IN13 by means of the

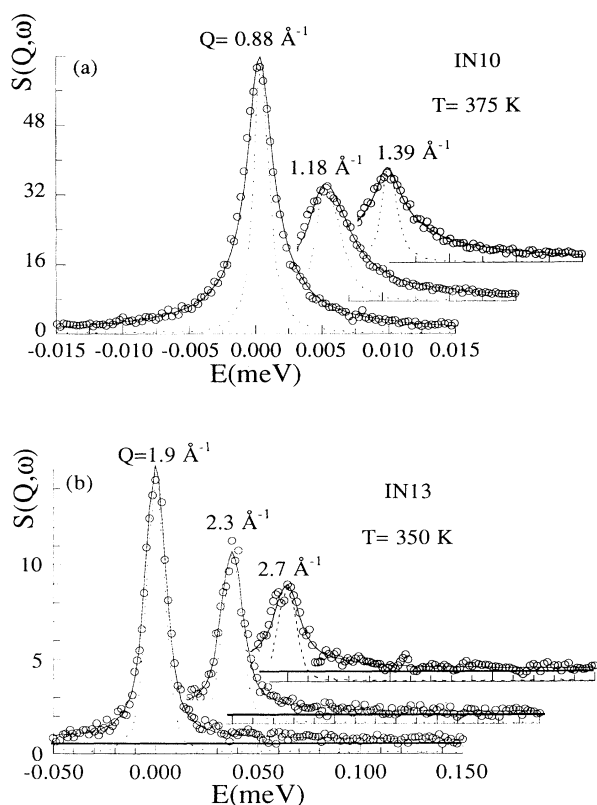


FIG. 5. Different fittings of PVME  $S(Q, \omega)$  measured by (a) IN10 and (b) IN13. Solid lines are the fitting curves obtained through the HN function with  $\alpha=0.68$  and  $\gamma=0.65$ . The measured resolutions are also shown for comparison (dotted lines). Thick lines correspond to the flat background used.

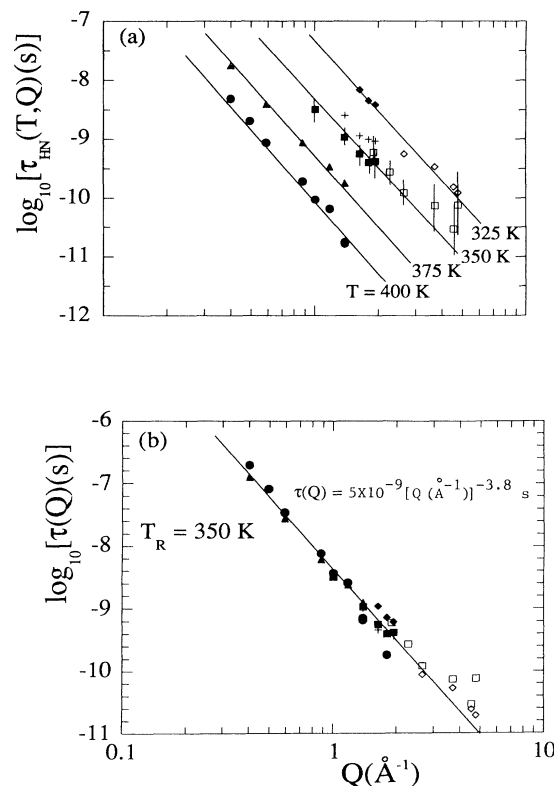


FIG. 6. (a)  $Q$  behavior of the HN relaxation times obtained from the fitting of  $S(Q, \omega)$  at several temperatures: 325 K ( $\blacklozenge$ ) (IN10), 325 K ( $\blacklozenge$ ) (IN13), 340 K ( $+$ ) (IN10), 350 K ( $\blacksquare$ ) (IN10), 350 K ( $\square$ ) (IN13), 375 K ( $\blacktriangle$ ) (IN10), and 400 K ( $\bullet$ ) (IN10). Solid lines describe a  $Q^{-4}$  law for comparison. (b)  $\tilde{\tau}(Q)$  master plot at a reference temperature of 350 K. The solid line is a linear regression fit showing the  $Q$  dependence of HN relaxation times.

theoretical scattering law  $S(Q, \omega)$  [Eq. (6)] plus the FBG, previously convoluted with the experimental energy-resolution function of the spectrometer. Some examples of the fitting procedure described above are shown in Fig. 5. As can be seen, the theoretical fitting curves convoluted with the resolution function describe very well the experimental data obtained by both IN10 and IN13 spectrometers. The values of  $\tau_{\text{HN}}(Q, T)$  obtained from the above-described fitting of the experimental spectra have been plotted in Fig. 6(a) as a function of  $Q$ . It is important to point out that the values of  $\tau_{\text{HN}}(Q, T)$  obtained at the same temperature and same  $Q$  range but from different spectrometers (i.e., different dynamical ranges) agree reasonably well. This supports the validity of the fitting procedure described above.

#### IV. DISCUSSION

Figure 6(a) shows the  $Q$  dependence of the  $\tau_{\text{HN}}$  value obtained from the fitting procedure at different temperatures. The overall errors in the obtained  $\tau_{\text{HN}}(Q, T)$  are difficult to estimate, since there is a number of contributing factors. These include the error in the actual measurement, the error in the fitting procedure as well as the error associated with the chosen theoretical  $S(Q, \omega)$ . An estimation of the first two are straightforward and are within the range of 10% of the resolution function. Errors associated with the chosen model are much more difficult to estimate. In any case an additional criterion followed by us was that data from the two different spectrometers, IN10 and IN13, i.e., different resolutions and energy “windows” yield compatible results for  $\tau_{\text{HN}}(Q, T)$ . Error bars showing the typical overall errors estimated by us have been drawn for 350-K data in Fig. 6(a).

As can be seen in the figure, the  $Q$  behavior of  $\tau_{\text{HN}}(Q, T)$  is almost independent of the temperature at least in the temperature range measured and inside the experimental errors involved. Then, this implies that  $\tau_{\text{HN}}(Q, T)$  can be factorized as  $\tau_{\text{HN}}(Q, T) = a(T)\check{\tau}(Q)$ . A master curve  $\check{\tau}(Q)$ , given the  $Q$  dependence of  $\tau_{\text{HN}}(Q, T)$ , can be built by shifting the  $\tau_{\text{HN}}(Q, T)$  values in the logarithmic  $\tau$  scale towards the reference values  $\tau_{\text{HN}}(Q, T_R)$ . Here  $T_R$  is an arbitrary temperature of reference included in the temperature range measured. Moreover, the shift factor values used for producing this master curve, allow to obtain the  $a(T)$  behavior and therefore the temperature dependence of  $\tau_{\text{HN}}(Q, T)$ . The obtained master curve  $\check{\tau}(Q)$  is shown in Fig. 6(b) where we have used  $T_R = 350$  K. The solid line in the figure is a linear regression fit of logarithmic  $\check{\tau}(Q)$  versus  $\log_{10} Q$ . From this fit the  $Q$  dependence of  $\tau_{\text{HN}}(Q, T)$  can be described by a power law  $\check{\tau}(Q) \propto Q^{-n}$  with an average value of  $n$  near 4. A similar experimental result was reported by Allen *et al.* for poly(dimethyl siloxane).<sup>26</sup> A law  $\check{\tau}(Q) \propto Q^{-4}$  was deduced by de Gennes when he calculated the incoherent scattering law  $S(Q, \omega)$  corresponding to a Rouse chain.<sup>27</sup> However, the  $Q$  values covered in both, the work reported in Ref. 26 and ours, lie largely in the range  $Q\sigma > 1$  ( $\sigma$  is the distance between beads in the Rouse model and is estimated to be  $> 10$  Å for most po-

lymers) where the calculations of de Gennes are unrealistic.<sup>27</sup> For this reason, the possibility that the found  $Q$  behavior corresponds to a Rouse-like dynamics should be discarded in our opinion. One could think that the found  $Q$  behavior should be very dependent on the chosen flat background. This could be very possible in the case of IN13 measurements but not in the case of IN10 measurements where the FBG value, if any, is very low and the values of the relaxation times obtained do not seem to be very affected by the chosen flat background. Figure 6(a) shows that the relaxation times corresponding to IN10 measurements also follow a law close to  $\check{\tau}(Q) \propto Q^{-4}$  independently of the IN13 values. Therefore, under the assumption that the above-mentioned separation into FBG and relaxation spectrum is valid, the observed  $Q$  dependence for relaxation times should be due to the  $\alpha$  process. We are now testing this behavior in several polymers and the results will be the subject of a future paper.

We now compare the temperature dependence of  $\tau_{\text{HN}}(Q, T)$ , which is given by  $a(T)$ , to the temperature behavior of the HN relaxation times obtained from dielectric, mechanical, and nuclear-magnetic-resonance spectroscopies (Fig. 7). It is clear that the values of  $\tau_{\text{HN}}(T)$  obtained by different relaxation experimental techniques have not only the same temperature behavior, very different to the one corresponding to an activated relaxation process, but also similar absolute values. Therefore the temperature behavior of the relaxation times controlling dielectric, mechanical, and NMR can be parametrized by only one law. We have parametrized this behavior by means of a Vogel-Fulcher law:

$$\tau_{\text{HN}}(T) = 1.3 \times 10^{-13} \exp \left[ \frac{1782K}{T - 189K} \right] \text{ s} . \quad (7)$$

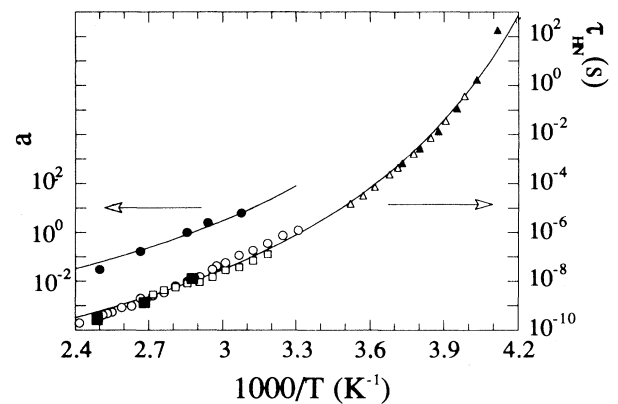


FIG. 7. Temperature behavior of the HN relaxation times for the  $\alpha$  process of PVME obtained by mechanical ( $\blacktriangle$ ), dielectric ( $\triangle$ ), and NMR ( $\circ$  and  $\square$ ) measurements. The solid line is the Vogel-Fulcher fit given by Eq. (7). Solid squares represent neutron-scattering relaxation time values at constant  $Q=0.85$  Å $^{-1}$ . The figure also shows the  $a(T)$  values ( $\bullet$ ) used to build the  $\check{\tau}(Q)$  master plot. The solid line through the  $a(T)$  points is also given by Eq. (7) but shifted in the time scale.

As can be seen in the figure, the Vogel-Fulcher law fits very well the temperature dependence of the characteristic time  $\tau_{\text{HN}}$  of the macroscopic  $\alpha$  relaxation. Moreover, as Fig. 7 displays, the same law also fits the  $a(T)$ , i.e., the temperature dependence of the HN relaxation times, obtained from neutron-scattering measurements.

The Vogel-Fulcher law used [Eq. (7)] is equivalent to a Williams-Landel-Ferry (WLF) equation given by

$$\log_{10}[\tau_{\text{HN}}(T)] = \log_{10}[\tau_{\text{HN}}(T_g)] - \frac{c_1(T - T_g)}{c_2 + T - T_g} \quad (8)$$

with the following WLF parameter values:  $c_1 = 12.7$ ;  $c_2 = 61$  K. These values are similar to the reported ones in Ref. 21 corresponding to only dielectric measurements in PVME. They are also in the range commonly obtained for different polymers.<sup>28</sup> However, they are not very close to the so called “universal” ones ( $c_1 = 17.5$ ;  $c_2 = 52$  K).<sup>28</sup>

From the results summarized in Figs. 6 and 7 we can also have an estimation about the “predominant”  $Q$  in the relaxation measurements. In the temperature range covered by neutron scattering (325–400 K), the values of  $\tau_{\text{HN}}(Q, T)$  at a  $Q$  value of about  $0.85 \text{ \AA}^{-1}$  are similar to the values of  $\tau_{\text{HN}}(T)$  measured by the NMR technique (see Fig. 7). Thus, we can define a “predominant spatial scale” for the dynamics of the  $\alpha$  process as it is observed by relaxation techniques. This should be of the order of  $\zeta \sim Q^{-1} = 1.2 \text{ \AA}$ . Taking into account the spatial structure of the PVME monomer and the values of both, bond lengths and angles, the found value of  $\zeta$  lies in the range one can expect for some molecular motions or conformational jumps.<sup>23</sup> In any case this will be the subject of future studies.

From the above-mentioned results, we can see that the parameters  $\alpha$  and  $\gamma$  have similar values for all the experimental techniques used. Figure 8 shows the time-domain correlation functions obtained by Fourier transform of the HN relaxation functions used to fit dielectric, mechanical, NMR, and neutron-scattering data. It is clearly shown that in all cases the time decay describing the stretching of the  $\alpha$  relaxation, can be described very well by the same stretched exponential with a  $\beta$  value of 0.44. Moreover, the fact that the temperature behavior of the characteristic HN relaxation time obtained from different probes is the same proves that the different susceptibilities obtained by different spectroscopies (dielectric, mechanical, NMR, and quasielastic neutron scattering) in a wide frequency range ( $10^{11} - 10^{-2} \text{ s}^{-1}$ ), ranging from mesoscopic to macroscopic time scales, can be scaled by using shift factors which follow the same temperature behavior, i.e., the dynamics of the  $\alpha$  relaxation shows universality.

Some implications of these results concern to the predictions of the mode coupling theory of the dynamics of glass-forming liquids.<sup>5,7</sup> This theory predicts the existence of a dynamic instability at some critical temperature  $T_c$  above the experimental glass transition ( $T_c \sim T_g + 40$  K). The main magnitude of this theory is

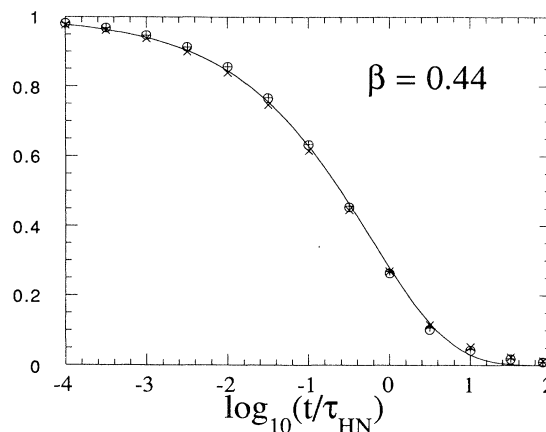


FIG. 8. Time-domain decay behavior obtained by Fourier transformation of the dielectric (x), mechanical (O), and NMR (+) HN fits. The solid line corresponds to a stretched exponential with  $\beta = 0.44$ .

the density correlation function. Above  $T_c$  this magnitude should perform a two-step decay. A fast local motion (called the  $\beta$  process, although with a different meaning to what is usually referred to as a  $\beta$  process in polymer science) is followed by the primary  $\alpha$  process. With decreasing temperature the  $\alpha$  process is slowed down dramatically until it does not occur below  $T_c$ . These predictions should imply a change in the temperature behavior of the experimental characteristic time scale of the dynamics close to  $T_c$ .

In spite of the finding of universality for the  $\alpha$  relaxation predicted by the mode-coupling theory, the results presented here for PVME give no direct hint for a critical temperature from the temperature behavior of the characteristic time scale of the  $\alpha$  process as it is measured by different probes. In fact such a behavior is predicted by the nonidealized mode-coupling theory<sup>7</sup> where the dynamical processes which restore ergodicity at temperatures below the critical one,  $T_c$ , are accounted for. But, even in this case we would guess to find a change for the relaxation time behavior with temperature and/or the spectral shape around  $T_c$ . Otherwise, we cannot distinguish the processes restoring ergodicity below  $T_c$  from the  $\alpha$  relaxation dynamics. However, in the case of PVME as it has been above mentioned we can describe the dynamics in a wide temperature range from  $T_g - 5$  K to  $T_g + 150$  K by using the same spectral shape.

## V. CONCLUSIONS

The main conclusion of this paper is that, at least in the case of PVME, the dynamics above the glass transition in a wide time range ( $10 - 10^{-10}$  s) can be well described by using the same “spectral shape,” i.e., similar

Havriliak-Negami parameters or close equivalent  $\beta$  values of the stretched exponential functions. Moreover, the characteristic time scale  $\tau_{\text{HN}}$  deduced from these fits can also be described by using only one Vogel-Fulcher (or equivalently one Williams-Landel-Ferry) functional form. Thus, this implies a self-consistent description of the dynamics obtained by very different probes.

#### ACKNOWLEDGMENTS

This work was supported in part by the Universidad del País Vasco—Euskal Herriko Unibertsitatea EHU Project No. UPV89 COD. 206.215-0029/89, and by CI-CYT Project No. MEC MAT89-0186. We also thank Gipuzkoako Foru Aldundia for partial financial support.

- <sup>1</sup>Several papers in *Molecular Dynamics and Relaxation in Glasses*, edited by Th. Dorfmueller and G. Williams (Springer-Verlag, Berlin, 1987).
- <sup>2</sup>*Polymer Motion in Dense Systems*, edited by D. Richter and T. Springer (Springer-Verlag, Berlin, 1988).
- <sup>3</sup>*Dynamics of Disordered Materials*, edited by D. Richter, A. J. Dianoux, W. Petry, and J. Teixeira (Springer-Verlag, Berlin, 1989).
- <sup>4</sup>*Basic Features of the Glassy State*, edited by J. Colmenero and A. Alegria (World Scientific, Singapore, 1990).
- <sup>5</sup>E. Leutheusser, *Phys. Rev. A* **29**, 2665 (1984).
- <sup>6</sup>U. Bengtzelius, W. Götze, and A. Sjoelander, *J. Phys. C* **17**, 5915 (1984).
- <sup>7</sup>W. Götze, in *Liquids, Freezing and the Glass-Transition*, (Proceedings of the Les Houches Summer School, Course LI, July 1989, edited by D. Levesque, J. P. Hanse, and J. Zim-Justin (North-Holland, Amsterdam, in press).
- <sup>8</sup>F. Mezei, W. Knaak, and B. Farago, *Phys. Rev. Lett.* **58**, 571 (1987).
- <sup>9</sup>D. Richter, B. Frick, and B. Farago, *Phys. Rev. Lett.* **61**, 2465 (1988).
- <sup>10</sup>B. Frick, *Prog. Colloid Polym. Sci.* **80**, 164 (1984).
- <sup>11</sup>W. Petry, M. Kiebel, and H. Sillescu, in *Dynamics of Disordered Materials*, edited by D. Richter, A. J. Dianoux, W. Petry, and J. Teixeira (Springer-Verlag, Berlin, 1989), p. 58.
- <sup>12</sup>W. Doster, S. Cusak, and W. Petry, *Phys. Rev. Lett.* **65**, 1080 (1990).
- <sup>13</sup>J. Colmenero, A. Alegria, and B. Frick, in *Basic Features of the Glassy State*, edited by J. Colmenero and A. Alegria (World Scientific, Singapore, 1990) p. 257.
- <sup>14</sup>J. Colmenero, A. Alegria, J. M. Alberdi, and B. Frick, *J. Non-Cryst. Solids* **131-133**, 949 (1991).
- <sup>15</sup>*Handbook of Chemistry and Physics*, edited by R. C. Weast and M. J. Astle (Chemical Rubber Company, Boca Raton, FL, 1983).
- <sup>16</sup>S. Havriliak and S. Negami, *J. Polym. Sci. C* **14**, 99 (1966).
- <sup>17</sup>K. S. Cole and R. H. Cole, *J. Chem. Phys.* **9**, 341 (1941).
- <sup>18</sup>D. Davidson and R. H. Cole, *J. Chem. Phys.*, **19**, 1484 (1951).
- <sup>19</sup>G. Meier, B. Gerharz, D. Boese, and E. W. Fischer, *J. Chem. Phys.* **94**, 3050 (1991).
- <sup>20</sup>F. Alvarez, A. Alegria, and J. Colmenero, *Phys. Rev. B* **44**, 7306 (1991).
- <sup>21</sup>A. Zetsche, F. Kremer, W. Jung, and H. Schulze, *Polymer* **31**, 1833 (1990).
- <sup>22</sup>M. Jehring, *Principles of High Resolution NMR in Solids* (Springer-Verlag, Berlin, 1983), Chap. 8.
- <sup>23</sup>R. Dejean de la Batie, F. Lauprete, and L. Monnerie, *Macromolecules* **21**, 2045 (1988).
- <sup>24</sup>B. Frick, D. Richter, and L. Fetters, in *Basic Features of the Glassy State*, edited by J. Colmenero and A. Alegria (World Scientific, Singapore, 1990), p. 204.
- <sup>25</sup>F. Fujara and W. Petry, *Europhys. Lett.* **4**, 921 (1987).
- <sup>26</sup>G. Allen, J. S. Higgins, A. Macounachie, and R. E. Ghosh, *Chem. Soc. Faraday Trans. II* **78**, 2117 (1982).
- <sup>27</sup>P. G. de Gennes, *Physics* **3**, 37 (1967).
- <sup>28</sup>*Viscoelastic Properties of Polymers*, 3rd ed., edited by J. D. Ferry (Wiley, New York, 1980).